

The precision of the sea surface temperature  
via NOAA-AVHRR sensor

Ryuzo Yokoyama, Sumio Tanba,  
Takashi Souma, Isao Yoshida  
Dept. of Computer Science,  
Faculty of Engineering, Iwate Univ.  
4-3-5, Ueda, Morioka, Iwate, Japan 020

## 1. Introduction

The Advanced Very High Resolution Radiometer (AVHRR) has been aboard NOAA series of sun-synchronous polar orbiting satellites after NOAA-6. Since the sensor can observe the earth surface twice in a day with 3,000 km of the swath width and 0.1°C of the temperature resolution, sea surface temperature (SST) images produced from their thermal infrared data have been conveniently used in the oceanography. The AVHRR has three thermal infrared channels which are at 3.5-3.9 $\mu$ m (ch. 3), 10.5-11.5 $\mu$ m (ch. 4) and 11.5-12.5 $\mu$ m (ch. 5), although the last one is only available on the satellites with odd numbers, presently on NOAA-7 and NOAA-9. The field accuracy of the estimated SST is limited by systematic and random errors stemming from improper sensor calibrations, contaminations in optical systems, atmospheric effects, air-sea interacting effects, etc.

A number of papers, e.g., *Maul and Sidran* (1970), *Prabhakara et al.* (1974), *McMillin* (1975), *Deshamps and Phulphin* (1980), etc, have been concerned with theoretical investigations about the atmospheric effects, which are specific to each thermal infrared band. Owing to those approaches, an SST estimation algorithm called a multi-channel sea surface temperature method (MCSST) has been developed. The SST estimation functions by the MCSST have a fundamental structure as weighted sum of the brightness temperatures of the AVHRR. The coefficients depend upon the atmospheric contents.

On the other hand, thermal radiations from the sea surface depend upon the skin temperature and the emissivity, which are affected by various air-sea interacting effects. *Robinson et al.* (1984) reviewed the present states of research. Relevant error correction algorithms, however, are not known for this kinds of disturbances.

By assuming error occurrence processes to be in a black box, experimental approaches have been carried out to compare the brightness temperatures with in situ SST and to determine coefficients in the MCSST. The derived estimation function can be effective not only for errors of atmospheric effects but also of all kinds. The data processing procedure for producing an SST estimation map from AVHRR data is very simple, once a reasonable estimation function is determined.

By using 82 ship and buoy SST data mostly in the tropical Pacific, *Bernstein* (1982) got an estimation function with the standard error (standard deviation of residues) was 0.6°C. The in situ SSTs were claimed to be accurate to  $\pm 0.2^\circ\text{C}$  and coincident to AVHRR SST within 100km and several days. *McClain et al.* (1982) and *Strong et al.* (1984) reported other validation tests by using another in situ SST data mostly in Southern Hemisphere. In the results of Strong, the standard error by using the drifting buoy data of coincidence within 24h and 50km was 0.68°C. For the case of the daytime data only, the standard error reduced to

0.49°C.

Resulting estimation functions partially depend upon the characteristics of the test data set, which are affected by accuracy of measurements, regional and temporal factors, etc. More case studies are necessary to evaluate and improve the MCSST, but only a limited number of papers have appeared at present. The main reason comes from difficulties to collect matching-up in situ SST data of high accuracy, good coincidence, a rather wide and even data distribution to guarantee the quality of analyses.

This paper is concerned with another case study of the MCSST by using in situ SST provided by fixed buoys in Mutsu bay of northern Japan. The accuracy and the coincidence of the data set, however, is excellent as stated in the later. In what follows, outlines of the buoy system and the data set assembling procedures are described. Both the single variate and the double variate regression analyses were applied to three grouped data sets, i.e., the total data, the daytime data, the nighttime data. Furthermore, estimation functions of *McClain et al.* (1982) and *Strong et al.* (1984) were applied to our daytime data set. Residues via those estimation functions have small biases, but their standard errors were just comparable to that of our regression function.

## 2. Data used in the analyses

### (a). In situ SST data

As shown in Fig. 1, Mutsu bay is situated in the northern end of Honshuu, Japan and has a size of about 50km×40km with a rather flat floor. Its deepest part is at the bay mouth and is about 50m bellow the sea surface. The bay has been utilized as cultivation fields of scallop, of which annual product is around 80 million dollars. Composed of six independent fixed buoys, the Mutsu bay automatic monitoring buoy system has been operating for these 6 years. At each buoy, items listed in Tab. 1 are measured every hour on the hour and the data have been stored in a data base. Pt. resistance detectors are implemented in the temperature measurement devices, which is claimed to be accurate to  $\pm 0.1^\circ\text{C}$  in the manual. The temperature data at 1m depth were used as in situ SST data.

### (b). AVHRR SST data

The AVHRR data were supplied by Institute of Industrial Science, Tokyo University. At the data receiving station there, almost AVHRR data of its overpath have been stored for these five years. Unfortunately, ch. 3 data were suffered from severe noises caused by electrical troubles in the sensors, and we were directed to use only ch. 4 and ch. 5 data in the subsequent analyses.

The brightness temperatures in the match-up data set were required that pixels in the vicinity of each buoy position were cloud-free, noise-free and in smaller horizontal temperature gradients. The last one is to keep the sensitivity of the temperature fluctuation minimum due to slight misidentifications of the buoy positions.

By roughly visual checks, 22 images in which clouds were free around the bay (including partially free) were selected out of the accumulated AVHRR data of NOAA-7 and NOAA-9. The list is shown in Tab. 2. Each image was geometrically corrected by the

oblique conformal secant conic projection. Then buoy positions were identified according to their latitude and longitude coordinates. Since Mutsu bay has a strongly closed geographical structure, a number of capes around were served as distinctive ground control points in the projections. Errors in the identification were evaluated within one pixel resolution which is about  $1.1\text{km}\times 1.1\text{km}$  at the nadir and  $1.5\text{km}\times 4.0\text{km}$  at the swath edge.

Both a visual inspection and an uniformity check were applied to pixels in the vicinity of each identified buoy position. In the visual inspection, images of ch. 2 and ch. 4 were displayed on a color CRT device ( $512\times 512$  pixels, 1 byte for 1 pixel of each channel) in an enlarged and high gain mode, and carefully observed around each buoy if pixels were contaminated by clouds or noises. In the uniformity check, the standard deviations of the brightness temperatures in the  $3\times 3$  pixels centered at each buoy position were calculated both for ch. 4 and ch. 5 data. When either of them were larger than  $0.2^\circ\text{C}$ , the buoy data were rejected from the test data set. The level of  $0.2^\circ\text{C}$  was determined intuitively as within two times of the AVHRR temperature resolution, but worked effectively.

Finally total number of 103 AVHRR SSTs at the buoys were screened out as the refined data. Among them, 85 cases were in the daytime and 18 cases in the nighttime. In the derivation of the brightness temperatures, we followed the algorithms described in *Lauritson et al.* (1979) for NOAA-7 data and in *Brown et al.* (1985) for NOAA-9 data.

The in situ SST data matching-up with those AVHRR SSTs were specified to be of the nearest time SST at each corresponding buoy. Since the measurement interval of the buoy data is one hour, the temporal coincidence in each match-up was within 30 minutes. The spatial coincidence is within one pixel resolution as stated previously.

Tab. 3 shows the statistics of the final match-up data sets in the three grouped cases. For all items of the mean, the standard deviation, the maximal and the minimal temperatures, in situ SST ( $y$ ) has the largest values. Then the brightness temperature of ch. 4 ( $x_4$ ) has the next, and that of ch. 5 ( $x_5$ ) is the smallest. Those might mainly come from the atmospheric attenuations of the thermal radiations.

Samples in the daytime data set diverge evenly in a wide range and form an appropriate data set for the test. The same situation is for the total data set, in which the daytime data are dominant in number. On the other hand, the nighttime data set has a specific data distribution in a narrow range, and the results should be understood just for references because of the particular data distribution.

### 3. Regression analyses

The regression analyses were applied to the match-up data sets both in the single variate and the double variates modes.

#### (a). Results of single variate regression analyses

The results are shown in Tab. 4. The scatter diagram in the result of ch. 4 is shown in Fig. 2. Let us look into the results of the total data set first. For both ch. 4 and ch. 5 cases, correlation coefficients are sufficiently high, but their slopes, intercepts, and residues appeared slightly different

owing to the different sensitivities to atmospheric effects. The standard error (standard deviation of the residues) in ch. 5 is about 0.25°C larger than that of ch. 4.

Large residues appeared to samples in the AVHRR data at 15:17 on 1984. 8. 10. when the buoy SSTs were 26~28°C, but their brightness temperatures were 19~20°C. According to the record of the Aomori meteorological station, the air-temperature, the relative humidity, the visibility, the wind velocity at that time were 29.9°C, 65%, 10km and 3.8m/s, respectively. That is, the weather around the bay was with high-temperature, high-humidity and weak-wind. In Japan, this kind of weather is very typical in summer. The large differences between in situ SST and brightness temperatures caused by a strong atmospheric effects were too large to be compensated by the single variate regression functions.

The results for the daytime data set were almost similar to those of the total data set. On the other hand, results of the nighttime data set were different from these two cases. This might come from its narrow data distribution and more match-up samples were needed to assert its generality.

(b). Results of double variates regression analyses.

Results are shown in Tab. 5. The standard errors were improved in comparison with the cases of the single variate analyses. The scatter diagram for the total data set is shown in Fig. 3. The samples in summer having large residues in the single variate analyses reduced remarkably. The different sensitivities of ch. 4 and ch. 5 to the atmospheric effects contributed for the better SST estimations. This should be the major advantage of the MCSST.

In the result of the total data set, however, other samples became prominent as having large residues. Those were in the AVHRR data at 3:09 on 1986.10.28. when the buoy SSTs and the brightness temperatures were 16.3~18.3°C and 12.1~13.5°C, respectively. According to the meteorological record at Aomori, the air-temperature, the relative humidity, the visibility and the wind velocity were recorded to be 5.2°C, 79%, 20km and 2.7m/s, respectively. The sky was very clear and the sea surface was calm. That is, the bay area was under a strong radiative cooling condition. There might exist large differences between the skin temperature and the 1m depth temperature of buoys. The large residues might be due to the air-sea interacting effects.

Residues were kept small in the results of the nighttime data set because of its specific data distribution such that samples occupied lower ends of the distribution and the regression function pierced them.

(c). Residues in other estimation functions

The available brightness temperatures in our data sets were restricted to ch. 4 and ch. 5 data due to the noise problem. But as long as the daytime SST estimation, the situation is the same in the MCSST because ch. 3 data are disturbed by the solar radiation reflecting at sea surfaces. How are the residues when the SST estimation functions by other authors are applied to our daytime data set? In *McClain et al.* (1982) and *Strong et al.* (1984), their SST estimation functions were described precisely. We calculated the statistics of residues due to the estimation functions. The results are shown in Tab. 6 including

our result.

There exist some negative biases (mean of residues) in the results by Strong's and McClain's, and their standard errors are just a little higher than that of ours. Our data set and their data sets (both McClain and Strong used in situ SST in the data base of the National Meteorological Center) were collected in different regions and by different methods. But those three results were consistent although the MCSST is a macroscopic method using the remotely sensed data from space. This should be a very interesting fact to demonstrate the generality of the MCSST.

#### 4. Conclusion

By regression analyses, the SST estimation functions by using ch. 4 and ch. 5 brightness temperatures of the AVHRR data were derived. The fixed buoy in Mutsu bay were used as in situ SSTs in the match-up data set. The total number of 103 match-up data were carefully screened out as cloud-free, noise-free and spatially stable samples. Their temporal and spatial coincidences are within 30 minutes and one pixel resolution. In the results of the single variate regression, standard errors for the total data set and the daytime data set were 1.2~1.5°C, in which large residues appeared to samples in summer under high-humidity conditions. In the double variate regression, the standard errors reduced to 0.8~1.0°C. In this case, large residues existed in samples under a strong radiative cooling condition.

By using our daytime data, errors were evaluated in the estimation functions of McClain and Strong. Then they were almost comparable to ours even though the estimation function were derived from the independent data sets.

The accumulation of the match-up data is still under way. Another extended results will be expected to appear in near future.

Acknowledgement: The authors should express garatitudes to Prof. Mikio Takagi, Institute of Industrial Science, Tokyo University for his providing us the NOAA-AVHRR data and to Aomori cultivation fishery center for the buoy data.

#### References

- Bernstein, R. L., Sea surface temperature estimation using the NOAA-6 satellite advanced very high resolution radiometer, *J. Geophys. Res.*, 87, 9455~9465, 1982.
- Brown, O. B., J. W. Brown and R. H. Evans, Calibration of advanced very high resolution radiometer infrared observations, *J. Geophys. Res.*, 90, 11,667~11,677, 1985.
- Deschamps, P. Y. and T. Phulpin, Atmospheric correction of infrared measurements of sea surface temperature using channels at 3.7, 11 and 12 $\mu$ m, *Boundary layer Meteorol.*, 18, 131~143, 1980.
- Lauritson, L., G. J. Nelson and F. W. Porto, Data extraction and calibration of TIROS-N/NOAA radiometers, NOAA Tech. Memo NESS 107, 1979.
- Maul, G. A. and M. Sidran, Atmospheric effects on ocean surface temperature sensing from the NOAA satellite scanning radiometer, *J. Geophys. Res.*, 78, 1909~1916, 1973.

- McClain, E. P., W. G. Pichel, C. C. Walton, Z. Amad and J. Sutton, Multi-channel improvements to satellite derived global sea surface temperatures, Reprint for XXIV Cospar meeting, Ottawa, A3. 1~11, 1982.
- McMillin, L. M., Estimation of sea surface temperatures from two infrared window measurements with different absorption, *J. Geophys. Res.*, 80, 5113~5117, 1975.
- Prabhakara, C., G. Dalu and V. G. Kunde, Estimation of sea surface temperature from remote sensing in the 11- to 13- $\mu$ m window region, *J. Geophys. Res.*, 79, 5039~5044, 1974.
- Robinson, I. S., N. C. Wells and H. Charnock, The sea surface thermal boundary layer and its relevance to the measurement of sea surface temperature by airborne and space radiometers, *Int. J. Remote sensing*, 5, 19~45, 1984.
- Strong, A. E. and E. P. McClain, Improved ocean surface temperatures from space, — Comparisons with drifting buoys —, *Bull. Am. Meteorol. Soc.*, 65, 138~142, 1984.

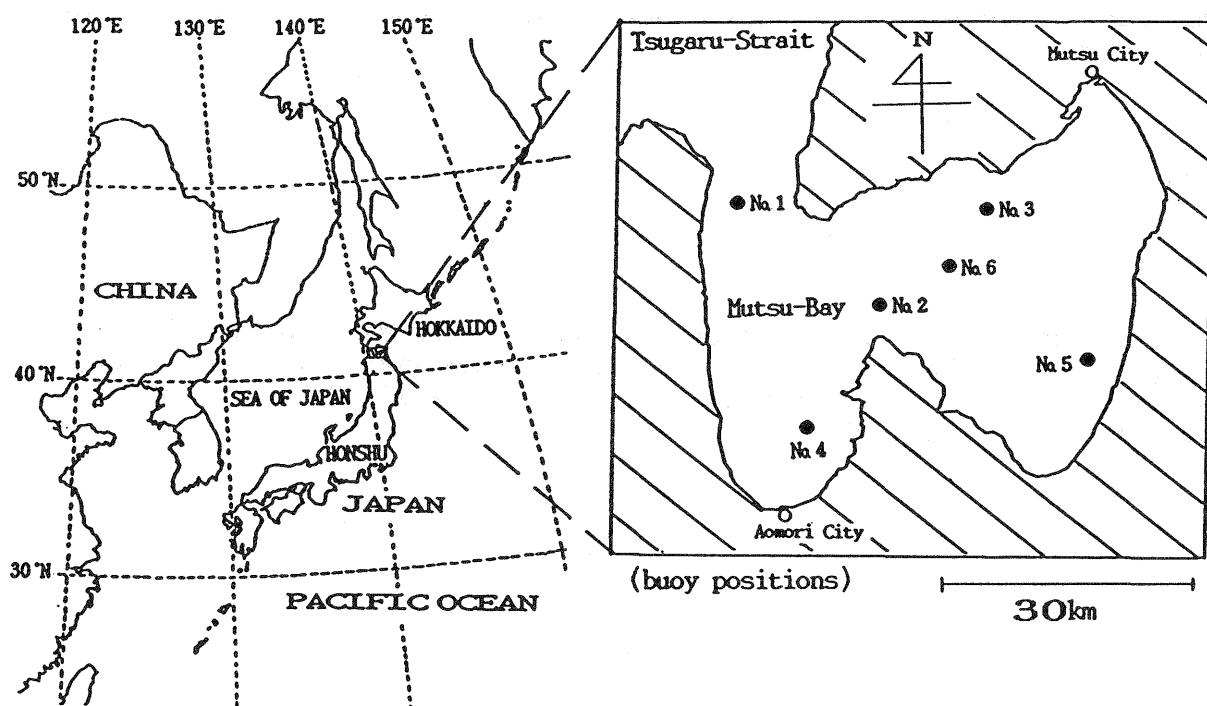


Figure 1 : Geographical location of Mutsu bay and positions of the fixed buoys.

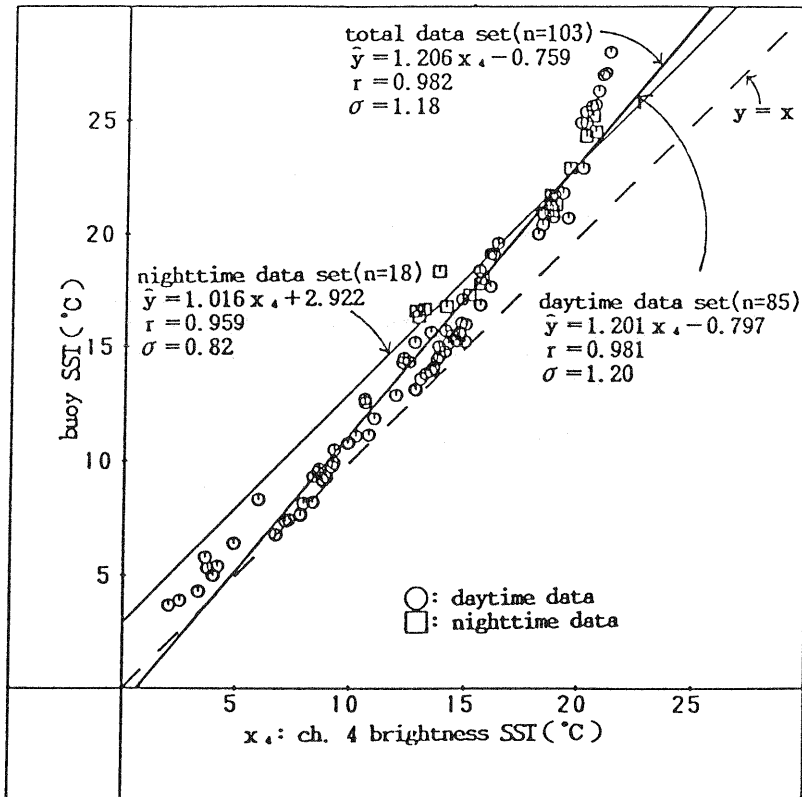


Figure 2 : Results of the single variate regression analysis for the three grouped data sets by using the ch. 4 brightness temperature.

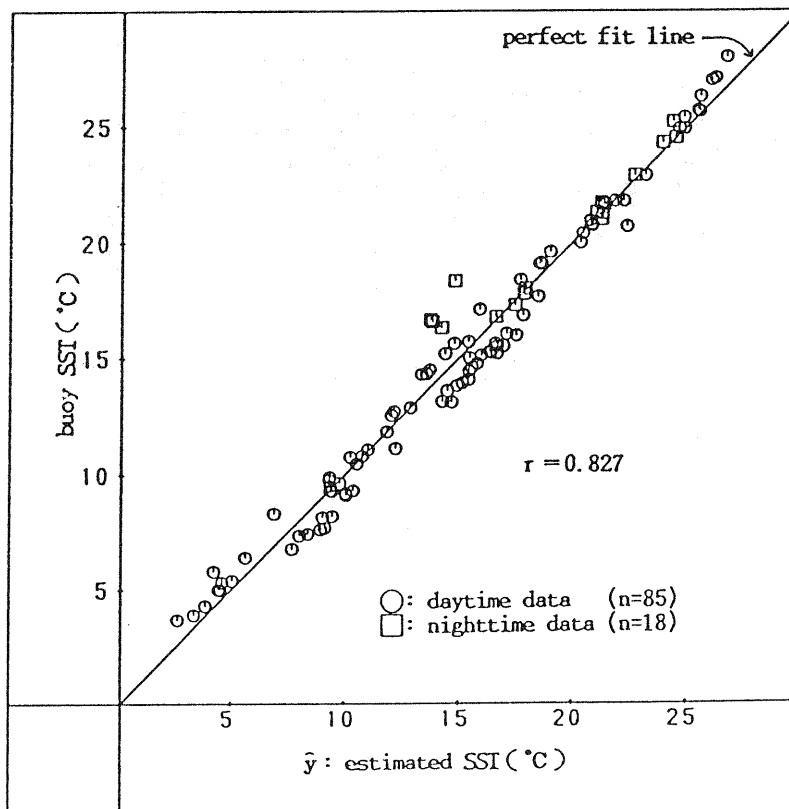


Figure 3 : Results of the double variate regression analyses by using the brightness temperatures of ch. 4 ( $x_4$ ) and ch. 5 ( $x_5$ ). The estimated SSI function is derived as  $\hat{y} = 1.117 x_4 + 2.71(x_4 - x_5) - 2.248$ .

Table 1 : Measurement items and depths of the buoys.

No.	Water Temp.	Salinity	Others
1	1m, 15m, 30m, 45m	1m, 15m, 30m, 45m	Flow: 15m, 45m
2	1m, 15m, 30m, 50m		
3	1m, 15m, 30m		
4	1m, 15m, 30m, 44m	1m, 15m, 30m, 44m	DO: 44m
5	1m, 15m, 36m		
6	1m, 15m, 30m, 46m	1m, 15m, 30m, 46m	DO: 30m, 46m Wind Air Temp.

Table 2 : List of Used NOAA Data.

NOAA-7		NOAA-9	
Date	Time	Date	Time
1984. 1. 29	14 : 52	1985. 4. 19	13 : 09
1984. 4. 24	14 : 02	1985. 4. 29	13 : 03
1984. 5. 19	13 : 56	1985. 5. 12	14 : 06
1984. 5. 25	14 : 22	1985. 10. 03	13 : 40
1984. 7. 20	14 : 35	1985. 10. 28	2 : 51
1984. 8. 2	3 : 35	1986. 4. 30	13 : 21
1984. 8. 6	14 : 26	1986. 6. 12	14 : 03
1984. 8. 10	15 : 17	1986. 6. 13	13 : 53
1984. 10. 15	15 : 06	1986. 9. 23	2 : 42
1984. 11. 9	14 : 58	1986. 10. 28	3 : 09
1984. 11. 16	15 : 12	1986. 11. 2	13 : 39

Time is meant the starting time of data reception in JSI at Institute of Industrial Science, Univ. of Tokyo.



Table 3 : Statistics of match-up data used in the regression analysis.

Data Set Specification	# of data	y (°C)				x <sub>4</sub> (°C)				x <sub>5</sub> (°C)			
		$\mu$	$\sigma$	max.	min.	$\mu$	$\sigma$	max.	min.	$\mu$	$\sigma$	max.	min.
Daytime Data Set	81	14.3	6.24	28.0	3.7	12.6	5.09	21.2	2.1	11.7	4.95	19.1	1.0
Nighttime Data Set	73	20.1	2.97	25.2	16.3	16.9	2.81	20.6	12.7	16.1	2.63	19.2	12.2
Total Data Set	154	15.4	6.20	28.0	3.7	13.3	5.04	21.2	2.1	12.4	4.91	19.2	1.0

$\mu$ : mean,  $\sigma$ : standard deviation, y: buoy SST, x<sub>4</sub>: ch. 4 brightness temp.,  
x<sub>5</sub>: ch. 5 brightness temp. All temperatures are described in °C.

Table 4 : Results of the single variate regression analysis by using the ch. 4 and ch. 5 brightness temperatures.

Data Set	# of data	Regression Function	Core. Coeff.	Residue (°C)		
				$\sigma$	max.	min.
Daytime Data Set	85	$\hat{y} = 1.201 x_4 - 0.797$	0.981	1.20	3.37	-1.86
		$\hat{y} = 1.224 x_5 + 0.062$	0.970	1.51	4.56	-2.15
Nighttime Data Set	18	$\hat{y} = 1.016 x_4 + 2.922$	0.959	0.82	1.51	-0.93
		$\hat{y} = 1.080 x_5 + 2.790$	0.953	0.87	1.76	-1.12
Total Data Set	103	$\hat{y} = 1.206 x_4 - 0.759$	0.982	1.18	3.23	-1.97
		$\hat{y} = 1.228 x_5 + 0.082$	0.973	1.43	4.45	-2.24

$\sigma$ : standard deviation,  $\hat{y}$ : estimated SST,  
x<sub>4</sub>: ch. 4 brightness temp., x<sub>5</sub>: ch. 5 brightness temp.  
All temperatures are described in °C.

Table 5 : Results of the double variate regression analysis by using the ch. 4 and ch. 5 brightness temperatures.

Data Set Specification	# of data	Regression Function	Core. Coeff.	Residue (°C)		
				$\sigma$	max.	min.
Daytime Data Set	85	$\hat{y} = 1.117 x_4 + 2.71(x_4 - x_5) - 2.248$	0.991	0.83	3.51	-1.67
Nighttime Data Set	18	$\hat{y} = 0.997 x_4 + 0.27(x_4 - x_5) + 2.990$	0.956	0.82	1.73	-1.47
Total Data Set	103	$\hat{y} = 1.146 x_4 + 2.10(x_4 - x_5) - 1.892$	0.987	0.98	1.52	-0.99

$\sigma$ : standard deviation,  $\hat{y}$ : estimated SST, x<sub>4</sub>: ch. 4 brightness temp.,  
x<sub>5</sub>: ch. 5 brightness temp. All temperatures are described in °C.

Table 6 : Statistics of residues provided by various SST estimation functions by using the daytime data set in Mutsu bay.

SST Estimation Functions	Bias	$\sigma$
Yokoyama et. al. (this paper): $y = 1.117x_4 + 2.71(x_4 - x_5) - 2.248$	0.000	0.827
McClain et. al. (1982) : $y = 1.035x_4 + 3.05(x_4 - x_5) - 1.215$	-0.319	0.910
Strong et. al. (1984) : $y = 1.035x_4 + 2.58(x_4 - x_5) - 0.604$	-0.491	0.937

$\sigma$ : standard deviation,  $\hat{y}$ : estimated SST, x<sub>4</sub>: ch. 4 brightness temp.,  
x<sub>5</sub>: ch. 5 brightness temp. All temperatures are described in °C.